JOM, Vol. 69, No. 10, 2017
DOI: 10.1007/s11837-017-2505-5

The Interface Structure of High-Temperature Oxidation–Resistant Aluminum-Based Coatings on Titanium Billet Surface

ZHEFENG XU,[1] JU RONG,[2] XIAOHUA YU,[2,4] MENG KUN,[2] ZHAOLIN ZHAN,[2] XIAO WANG,[2] and YANNAN ZHANG[3]

1.—Pan Gang Group Research Institute Co., Ltd., State Key Laboratory of Vanadium and Titanium Resources Comprehensive Utilization, Panzhihua 617000, China. 2.—National Engineering Research Center of Solid Waste Resource, Kunming University of Science and Technology, Kunming 650093, China. 3.—Faculty of Metallurgical and Energy Engineering, Kunming University of Science and Technology, Kunming 650093, China. 4.—e-mail: xiaohua_y@163.com

A new type of high-temperature oxidation-resistant aluminum-based coating, on a titanium billet surface, was fabricated by the cold spray method, at a high temperature of 1050°C, for 8 h, under atmospheric pressure. The microstructure of the exposed surface was analyzed via optical microscopy, the microstructure of the coating and elemental diffusion was analyzed via field emission scanning electron microscopy, and the interfacial phases were identified via x-ray diffraction. The Ti–Al binary phase diagram and Gibbs free energy of the stable phase were calculated by Thermo-calc. The results revealed that good oxidation resistant 50-μm-thick coatings were successfully obtained after 8 h at 1050°C. Two layers were obtained after the coating process: an Al_2O_3 oxidation layer and a $TiAl_3$ transition layer on the Ti-based substrate. The large and brittle Al_2O_3 grains on the surface, which can be easily spalled off from the surface after thermal processing, protected the substrate against oxidation during processing. In addition, the thermodynamic calculation results were in good agreement with the experimental data.

INTRODUCTION

The susceptibility of titanium and titanium alloys to oxidation, during heat-treatment processes, leads to the formation of a hard and brittle oxidation layer on the surface of these materials. This layer constitutes a waste (of up to 2.2%) of raw materials, and results in alloy-element dilution, economic loss and significant disruption to subsequent processing.[1–4]

Many researchers have developed various vacuum heat-treatment and inert gas (generally argon) protection technologies.[5] However, these technologies suffer from several drawbacks, which limit their use for various applications. For example, these methods are only suitable for small accessories, rather than the entire surface of large parts. High-temperature protective coatings have been fabricated in recent years in an attempt to overcome these drawbacks. These include glass-based and silicate coatings, which are used for pressing, extrusion, forging, rolling and heat-treatment processes.[6] However, the hydrolysis of glass and ceramic-based coatings is ineffective, and, hence, these coatings must be removed via alkaline or acid soaking, prior to cooking.[9] More importantly, owing to the strong bonding between titanium and oxygen, titanium atoms can remove the oxygen atoms from SiO_2.[7]

$TiAl_3$, which yields a protective Al_2O_3 film with self-repairing characteristics, has been reported in recent years.[8,9] This thin film is also compact and reliable.[10] In this work, aluminum powder (the main candidate) and additional ingredients such as Sn powder, SiO_2 powder, styrene acrylic emulsion, polyvinyl alcohol and carboxymethyl cellulose were used to fabricate oxidation–resistant aluminum-based coatings. The formation of high-temperature oxidation–resistant aluminum-based coatings on the surface of titanium billets, and the structure of the coating–billet interface, are essential for the application of titanium materials. Therefore, the high-temperature oxidation–resistant and interface

Zhefeng Xu and Ju Rong have contributed equally to this paper.

(Published online August 9, 2017)

structure of the coatings were analyzed via optical microscopy, field emission scanning electron microscopy and x-ray diffraction (XRD). Furthermore, in order to better analyyze the experimental results, the Ti–Al binary phase diagram and Gibbs free energy of stable phase were calculated by Thermo-calc.

EXPERIMENTAL

A Ti–4Al–2 V alloy was used as the substrate (dimensions: 100 × 50 × 20 mm, surface finish: 0.32 μm). The following procedure was performed, in order to obtain 1 L of the aluminum-based solution: (1) 10.50 wt.% styrene acrylic emulsion (solid content: 50%) was poured into a predetermined container; (2) 83.95 wt.% aluminum powder, 5.25 wt.% Sn powder (600 mesh), and deionized water were thoroughly mixed; (3) 0.12 wt.% SiO_2 (600 mesh), 0.06 wt.% polyvinyl alcohol and 0.12 wt.% carboxymethyl cellulose were then gradually injected into the container; and (4) the composite slurry was obtained by adding deionized water to 1 L.

The aluminum-based solution was sprayed (deposition rate: 1 μm/s) onto one side surface of the titanium alloy by the cold spray method (the development of low energy consumption, low-cost methods for protection of the Ti-alloy surface against oxidation during thermal processing is essential), using an automatic spray gun (006-1589), and 50-μm, 100-μm, and 150-μm-thick coatings were obtained. Thereafter, each coating was solidified after 8 h, under atmospheric pressure, in an annealing furnace at a constant high temperature of 1050°C (we chose this heat-treatment condition based on the overall hot rolling temperature and time).

After the heat treatment, an LSM 510 metallographic microscope was used to analyze the microstructure of the exposed surface. A JSM1600-LV scanning electron microscope and an inca energy spectrum analyzer were used to analyze the interface microstructure and elemental diffusion of the coating. A D/MAX-2200 x-ray diffractometer was used to characterize the interface of the coating.

RESULTS AND DISCUSSION

Morphology of the Exposed Surface

Ti-based alloys have a strong affinity for oxygen, and hence an oxidation scale forms on the surface (see Fig. 1a and b) after a high-temperature heat treatment. The pore- and crack-free surface coating, which is uniformly distributed on the substrate (see Fig. 1c), prevents scale formation (Fig. 1d). The crack-free surface is indicative of the strong adhesion between the coatings and the Ti-alloy substrate, as confirmed by the results of an adhesion test (under 980 N cm) on the coatings (Fig. 1e). A high-magnification image of the coatings (Fig. 1f) reveals the uniform size of the particles on the substrate.

The oxidation layer formed on the exposed surface (after 8 h, under atmospheric pressure, at a constant high temperature of 1050°C) is shown in Fig. 2 (the minimum thickness that can be achieved by the equipment is 50 μm). Figure 2a shows an 335-μm-thick oxide layer that formed on the titanium substrate. The oxide layer consists of relatively coarse particles: the internal oxidation layer, which forms along the grain boundary, penetrates deep into the substrate and has a needle-like morphology. This indicates that, during oxidation, oxygen atoms gradually penetrated the grain boundaries, which have high surface energy.

The surface of the ~330-μm-thick oxide layer (see Fig. 2b) contains only a few particles and the oxygen atoms extend further along the grain boundaries, compared to those associated with the ~335-μm-thick layer. Figure 2c shows a ~320-μm-thick oxide layer that formed on the titanium substrate. The degree of grain boundary oxidation is more severe than that observed in Fig. 2a and b, and the coarse surface of the oxide layer is replaced by a thin, sharp, internal oxide layer.

In contrast to oxidation of the exposed surface, oxidation of the titanium alloy started at the surface and progressed gradually toward the grain boundary, developing eventually into an entire layer. This layer broke and fell off after a certain degree of growth.

Surface Topography and Elemental Diffusion of the Coating

Figure 3 shows the results of the line scan performed on each sample (i.e., from the coating to the substrate), from which it can be seen that the titanium and aluminum content fluctuates significantly with increasing coating thickness. The samples can be divided into three layers, namely the high-temperature resistant coating, an intermediate layer and the titanium substrate, i.e., there is no obvious titanium oxide layer. Figure 3a shows that the aluminum content and oxygen content decreases from the coating surface to the interior. It can be inferred that the surface is mainly composed of Al_2O_3 phases. Figure 3b reveals considerably sharper fluctuations in the aluminum content and a more complex interface than that observed in Fig. 3a. This result illustrates that oxidation is more serious. According to the thermodynamic theory of materials,[11–14] the aluminum content has a significant influence on the interface and the corresponding product; therefore, the complexity of the interface increases with increasing coating thickness (and increasing fluctuation in the aluminum content). This is consistent with the

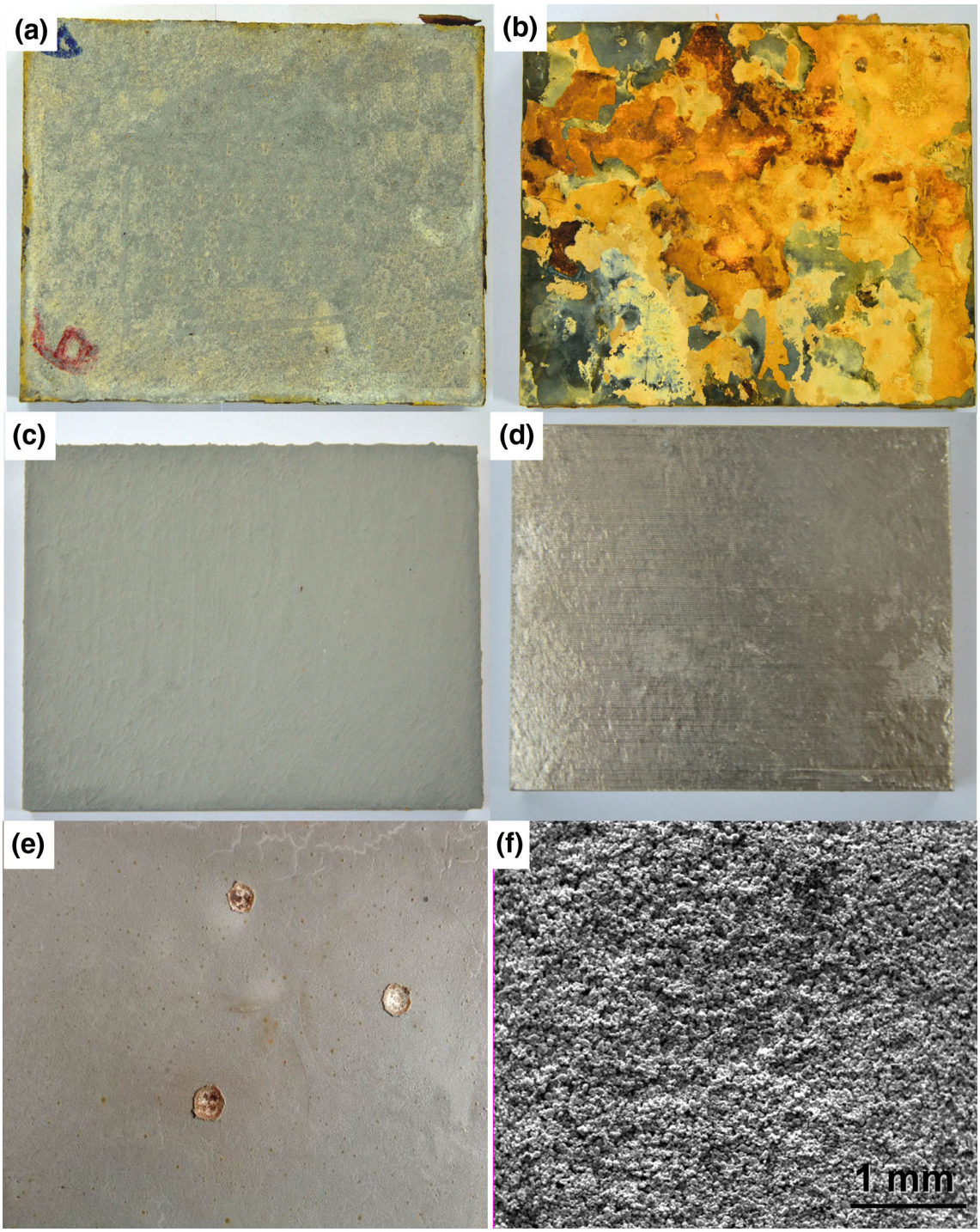

Fig. 1. Surface morphology of the: (a), (b) uncoated substrate before and after treatment; (c), (d) coated substrate before and after heat treatment; (e) crack-free surface after adhesion testing at 980 N cm. (f) High-magnification image of the surface coating on the substrate.

severe fluctuation in aluminum content and highly complex interface shown in Fig. 3c. Sharper fluctuations and complex interfaces are undesirable and must be avoided during the manufacturing process.[15–17] From the viewpoint of element content and interface complexity, the 50-μm-thick coating is the most desirable of the three types of coatings considered in this work.

Phase Analysis of the Coating

Figure 4 shows the XRD patterns of the high-temperature oxidation–resistant aluminum-based coatings (the phase composition and microstructure are independent of the coating thickness and hence, the 50-μm- and 150-μm-thick samples are compared). In addition, prior to the measurement, the

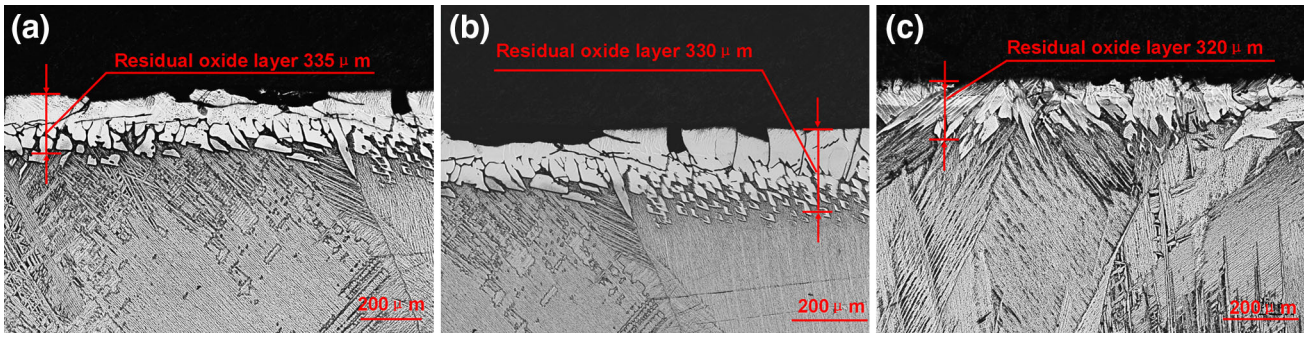

Fig. 2. Oxidation layer formed on the exposed surface. The samples shown in (a), (b) and (c) are, on average, 50 μm, 100 μm, and 150 μm thick, respectively.

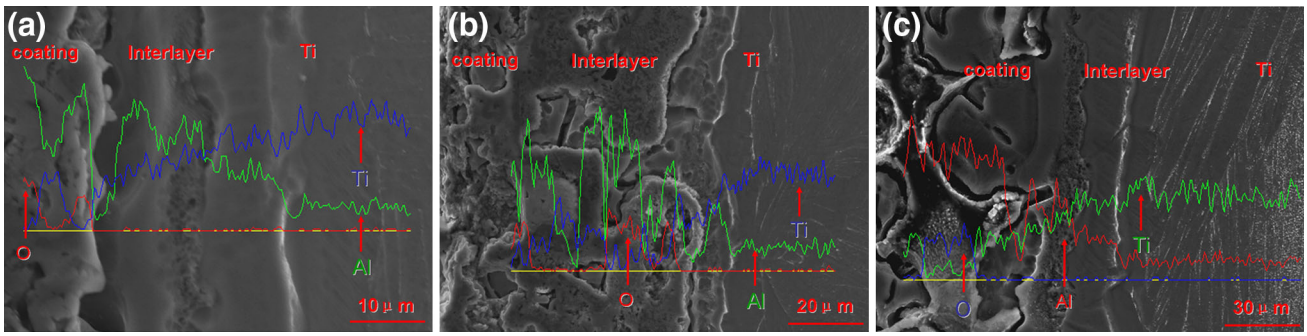

Fig. 3. Results of the line scan performed on each sample (i.e., from the coating to the matrix. The samples shown in (a), (b) and (c) are, on average, 50 μm, 100 μm, and 150 μm thick, respectively.

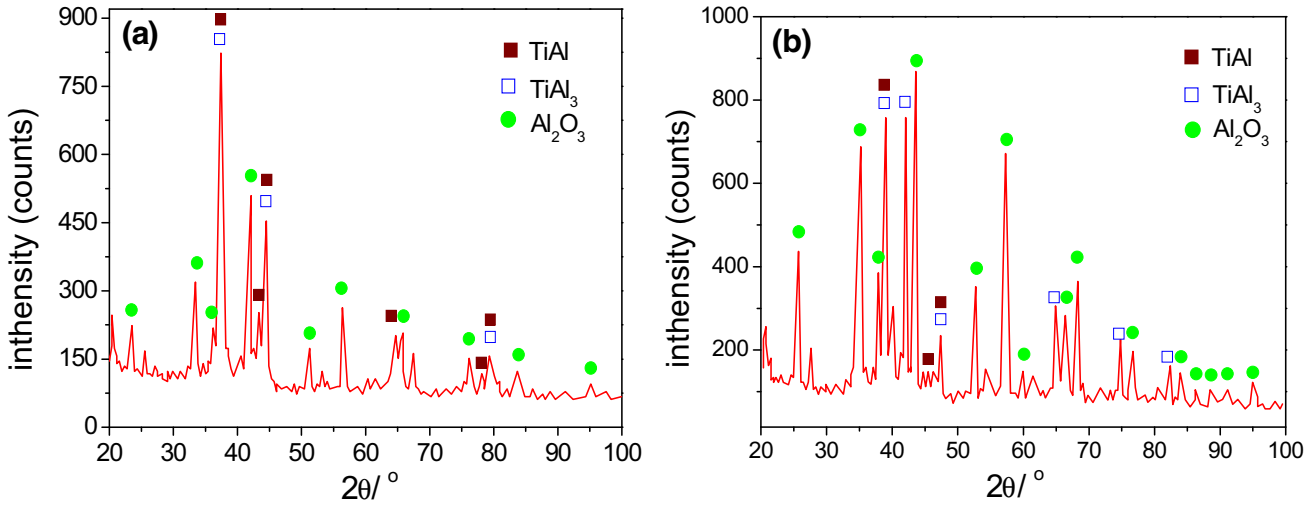

Fig. 4. X-ray diffraction patterns of high-temperature oxidation resistant aluminum based coatings; patterns obtained from samples that are, on average, (a) 50 μm and (b) 150 μm thick.

pattern needs to be treated with a stripping process. As the figure shows, the coating is composed primarily of $TiAl_3$, TiAl, and Al_2O_3 phases, but the characteristic peak of the pure aluminum phase is absent from the patterns. This indicates that the aluminum powder was oxidized to the dense Al_2O_3 phase during the heat treatment. This suggests that the aforementioned high-temperature oxidation–resistant aluminum-based coatings are composed of dense protective Al_2O_3, $TiAl_3$ and TiAl layers, which inhibit oxidation of the titanium billet.

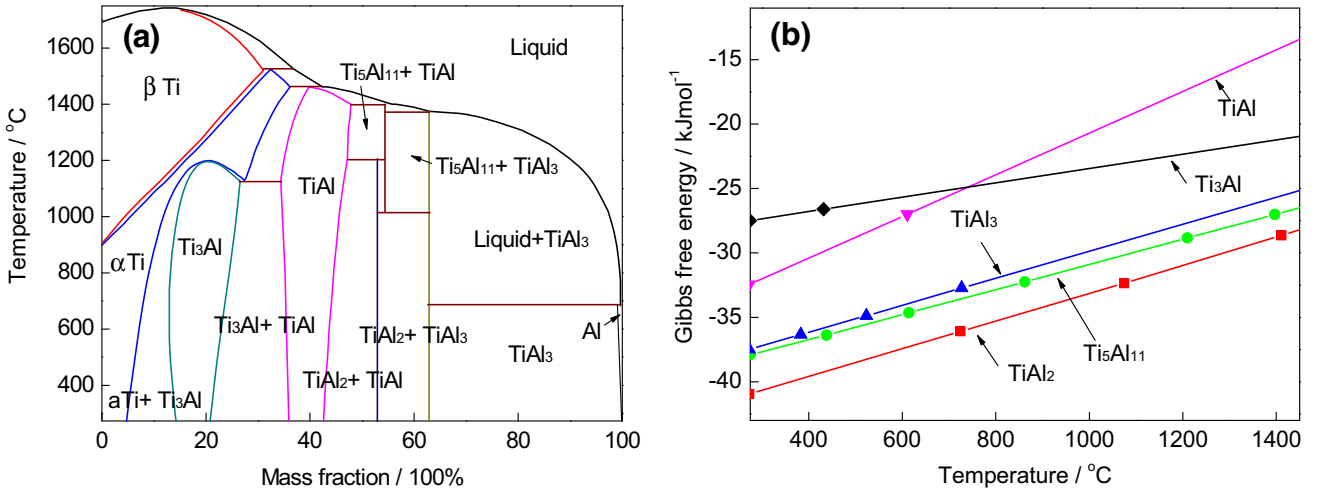

Fig. 5. Binary phase diagram and Gibbs free energy of Ti–Al intermetallic compounds: (a) Ti–Al binary phase diagram; (b) Gibbs free energy as a function of temperature.

According to the Ti–Al binary phase diagram (see Fig. 5a), Ti–Al intermetallic compounds, such as Ti_3Al, TiAl, $TiAl_2$, and $TiAl_3$, are stable at room temperature. Specifically, $TiAl_2$,[18] and Ti_5A1_{11} (or Ti_2A1_5[19,20]) can form at temperatures of 500–650°C, which are lower than the melting point (~660.4°C) of aluminum. Ti_5A1_{11} and $TiAl_2$ can precipitate from TiAl, but the Gibbs free energy of $TiAl_3$ is relatively lower than the Gibbs free energies of these compounds (as shown in Fig. 5b). Therefore, the Ti–Al intermetallic compounds may be listed in order of their ease of formation in the transition layer, i.e., $TiAl_3$ > TiAl > Ti_5A1_{11}. This result is in good agreement with the experimental data.

CONCLUSION

The cold spray method proposed in this work represents a new method for protecting the surface of titanium billets. A new type of high-temperature oxidation–resistant aluminum-based coating with self-repairing characteristics, on a titanium billet surface, is fabricated. The 50-μm-thick coating exhibits superior characteristics compared to the 100-μm and 150-μm-thick coatings. In addition, owing to the constituent co-existing Al_2O_3–TiAl layers and $TiAl_3$–Ti multilayers (agreeing well with the theoretical calculation), these coatings can effectively retard high-temperature oxidation of titanium billets during thermal treatments.

ACKNOWLEDGEMENTS

This work was supported by the Chinese National Science Foundation (Grants 51601081, 51665022 and 51165016).

REFERENCES

1. R. Pflumm, S. Friedle, and M. Schütze, *Intermetallics* 56, 1 (2015).
2. R.A. Yankov, A. Kolitsch, J.V. Borany, A. Mücklicha, F. Munnika, A. Donchevb, and M. Schützeb, *Surf. Coat. Tech.* 206, 3595 (2012).
3. M. Shen, P. Zhao, Y. Gu, S.L. Zhu, and F.H. Wang, *Corros. Sci.* 94, 294 (2015).
4. D.H. Qi, J.D. Yu, K. Gu, and Q. Ni, *Rare Mater. Met. Eng.* 1, 17 (1987).
5. J. Gao, Y. He, and W. Gao, *Thin Solid Films* 520, 2060 (2012).
6. T. Moskalewicz, F. Smeacetto, G. Cempura, L.C. Ajitdossb, M. Salvob, and C.A. Filemonowicz, *Surf. Coat. Tech.* 204, 3509 (2010).
7. S. Sarkar, S. Datta, S. Das, and D. Basu, *Surf. Coat. Tech.* 203, 1797 (2009).
8. T. Moskalewicz, F. Smeacetto, and A.C. Filemonowicz, *Surf. Coat. Tech.* 203, 2249 (2009).
9. S. Yılmaz, G. Bayrak, S. Senm, and U. Senb, *Mater. Des.* 27, 1092 (2006).
10. R.K. Dutta, R.M. Huizenga, M. Amirthalingam, A. King, H. Gao, M.J.M. Hermans, and I.M. Richardson, *Scripta Mater.* 69, 187 (2013).
11. L. Shi, C.S. Wu, and X.C. Liu, *J. Mater. Process. Technol.* 222, 91 (2015).
12. A. Arora, A. De, and T. DebRoy, *Scripta Mater.* 64, 9 (2011).
13. T. Moskalewicza, B. Wendlerb, F. Smeacettoc, M. Salvoc, A. Manescud, and A.C. Filemonowicza, *Surf. Coat. Tech.* 202, 5876 (2008).
14. D. Zheng, S. Zhu, and F. Wang, *Surf. Coat. Tech.* 200, 5931 (2006).
15. M. Chen, M. Shen, S. Zhu, F.H. Wang, and Y. Niu, *Mater. Sci. Eng. A* 528, 3186 (2011).
16. X.H. Yu, J. Rong, Z.L.L. Zhan, L. Liu, and J.X. Liu, *Mater. Des.* 83, 159 (2015).
17. X.H. Yu and Z.L. Zhan, *Nanoscale Res. Lett.* 9, 516 (2014).
18. H.Q. Li, Q.M. Wang, S.M. Jiang, J. Ma, J. Gong, and C. Sun, *Corros. Sci.* 53, 1097 (2011).
19. W. Li, M. Chen, C. Wang, S.L. Zhu, and F.H. Wang, *Surf. Coat. Technol.* 218, 30 (2013).
20. M. Chen, M. Shen, S. Zhu, F. Wang, and Y. Niu, *Mater. Sci. Eng.* 528, 3186 (2011).